Novel orthogonal modulation format DRZ-FSK/DPSK for high-speed long-haul optical communication

Junwen Zhang (张俊文), Yufeng Shao (邵宇丰), Wuliang Fang (方武良), Bo Huang (黄 博), Li Tao (陶 理), Jiangbo Zhu (朱江波) , and Nan Chi (迟 楠)*

State Key Lab of ASIC & System, Department of Communication Science and Engineering, Fudan University, Shanghai 200433, China

**E-mail: nanchi@fudan.edu.cn*

Received June 3, 2010

We propose a novel advanced orthogonal modulation format dark return-to-zero frequency shift keying/differential phase shift keying (DRZ-FSK/DPSK) and its realization scheme. The DRZ-FSK/DPSK is generated by the combination of a 40-Gb/s return-to-zero (RZ) signal and a DRZ signal which is converted from the RZ using a semiconductor optical amplifier (SOA) based on nonlinear cross polarization rotation (XPR) and then re-modulated by high-bit-rate DPSK at 40 Gb/s. The feasibility of the scheme is experimentally demonstrated. Bit error rate (BER) results of the total 80-Gb/s DRZ-FSK/DPSK orthogonal modulation signal with a subsequent 100-km single-mode fiber (SMF) transmission link show its potential for future high-speed long-haul optical communication.

OCIS codes: 060.2330, 060.4080.
doi: 10.3788/COL20100809.0852.

Recently, advanced modulation format techniques are a very hot research topic in high speed optical fiber communication for the robustness to chromatic dispersion and fiber nonlinear effects[1−4]. Among many modulation formats, the orthogonal modulation has attracted increased attention for its high spectrum efficiency[5]. A number of orthogonal modulation formats have been reported, including frequency shift keying (FSK) re-modulated with amplitude shift keying (ASK), differential phase shift keying (DPSK) with ASK, and dark return-to-zero (DRZ) with DPSK[6−11]. However, the bit rate of ASK modulation in these orthogonal modulation formats is usually very low, and most importantly, the optical signal intensity of the above orthogonal modulation formats is not constant, which reduces the robustness to fiber nonlinear effects[12].

Therefore, FSK re-modulated with DPSK could be a promising orthogonal modulation format in future high-speed and long-haul optical communication networks due to the high bit rate for both dimensions and the constant intensity. However, in conventional FSK transmitters based on direct modulation and electro-absorption modulation, the wavelength spacing between FSK tones and the modulation bit rate suffer from additional noise, driving current range, and response time limitations in semiconductors, so phase re-modulation is hard to implement[13−15].

In this letter we propose a novel scheme to realize the advanced orthogonal modulation format DRZ-FSK/DPSK. The DRZ-FSK is generated by the combination of return-to-zero (RZ) and DRZ which is converted from RZ using a semiconductor optical amplifier (SOA) as a nonlinear medium based on nonlinear cross polarization rotation (XPR). The feasibility of the scheme is experimentally demonstrated. The DRZ tone of the 40-Gb/s FSK signal is re-modulated with 40-Gb/s DPSK. The bit error rate (BER) results of the total DRZ-FSK/DPSK orthogonal modulation signal with a subsequent 100-km single-mode fiber (SMF) transmission link show potential for future high-speed long-haul optical communication.

The conceptual architecture of the proposed frequency/phase orthogonal modulation based on DRZ-FSK/DPSK realization is shown in Fig. 1. The first data stream is modulated as RZ-ASK and then split into two tributaries. The original RZ signal is expressed as

$$E_1(t) = \Big[\sum_{-\infty}^{+\infty} s_k q\Big(\frac{t-kT}{\tau}\Big)\Big] \cdot \exp[\mathrm{j}(2\pi f_1 t + \phi_1)],$$
$$s_k = 0, 1, \tag{1}$$

where s_k is the data of the original RZ signal, $q(\frac{t}{\tau})$ is the signal waveform shape of the RZ pulse with, τ is pulse width, and f_1 is the RZ signal frequency.

The RZ signal of the lower tributary is converted to DRZ based on XPR in the SOA followed by the DPSK

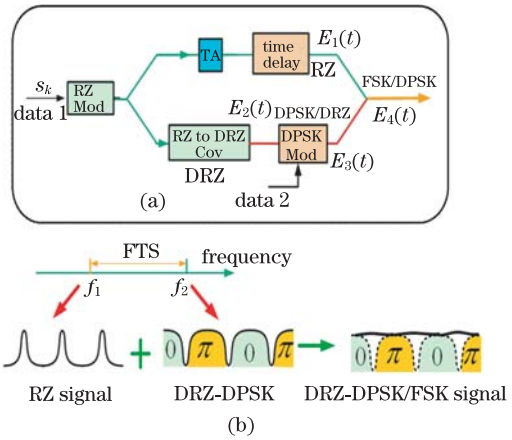

Fig. 1. (a) Conceptual architecture and (b) principle of the proposed orthogonal modulation DRZ-FSK/DPSK signal generation. Mod: modulator; Cov: converter; TA: tunable attenuato; FTS: frequency tone spacing.

modulator. The DRZ signal is

$$E_2(t) = \Big\{ \sum_{-\infty}^{+\infty} \Big[1 - s_k q\Big(\frac{t-kT}{\tau}\Big)\Big]\Big\} \cdot \exp\Big[\mathrm{j}(2\pi f_2 t + \phi_2)\Big]. \tag{2}$$

$E_2(t)$ is the DRZ signal which is inverted from the RZ signal with a wavelength conversion from f_1 to f_2 as we use wavelength conversion based on SOA here. We define

$$d_k(t) = 1 - s_k q\Big(\frac{t-kT}{\tau}\Big) \tag{3}$$

as the DRZ signal envelope waveform. Then the DRZ signal re-modulated by DPSK can be expressed as

$$E_3(t) = \sum_{-\infty}^{+\infty} d_k(t) \cdot \exp[\mathrm{j}(2\pi f_2 t + \phi_k(t)],$$
$$\phi_k(t) = 0, \pi, \tag{4}$$

where $\phi_k(t)$ is the differential phase of DRZ-DPSK signal for the kth bit. The principle of the DRZ-FSK/DPSK signal generation is illustrated in Fig. 1(b). The second data stream is modulated as DPSK on the DRZ signal which is clock aligned to each bit slot of the DPSK baseband signal. Combining it with the upper tributary RZ signal which is appropriately attenuated and time delayed, we can finally obtain the DRZ-FSK/DPSK orthogonal signal. The information is encoded in frequency/phase as expressed by

$$E_4(t) = \Big[\sum_{-\infty}^{+\infty} s_k q\Big(\frac{t-kT}{\tau}\Big)\Big] \cdot \exp[\mathrm{j}(2\pi f_1 t + \phi_0)] + \sum_{-\infty}^{+\infty} d_k(t) \cdot \exp[\mathrm{j}(2\pi f_2 t + \phi_k(t)]. \tag{5}$$

The operation principle of the proposed RZ to DRZ-FSK converter is shown in Fig. 2. The theoretical development of XPR has so far considered the nonlinear coupling either between two polarization components of a single optical field or between the identically polarized components of two optical fields at different frequencies. In this scheme, a continuous-wave (CW) light beam is fed into a SOA as a probe signal with a pumping RZ signal that is under strong input power. Before fed into the SOA, the polarizations of both laser beams are adjusted by polarization controller (PC) to 45° relative to each other. Under the condition, the two optical carriers undergo XPR within the SOA. When there is a RZ 'space' transmitted in the link, the probe signal can be selected by the polarizer that aligns in parallel in polarization. When the RZ signal is logical "1", oppositely, XPR in the SOA makes the probe laser partially invert in a polarization rotation angle. Combined with the orthogonal part, the probe signal cannot be detected by the polarizer because the output port has been rotated in a 90° angle. The result of this operation is a DRZ signal. Together with an appropriate delay of the RZ, we can obtain DRZ-FSK.

The system setup is shown in Fig. 3. The signal sources are one external cavity laser at 1557.3 nm. The first modulator generates a 40-GHz RZ pulse train with 33% duty cycle. The modulator is biased at the peak of its transmission curve and differentially driven at twice the switching voltage with an alternating current (AC) coupled half-bitrate (20 GHz) sine wave. The data at 40 Gb/s (pseudo-random bit sequence (PRBS) 2^{23}–1, ITU-T G.709 FEC) is generated by SHF BPG44E BT pattern generator and added onto the second MZM, thus

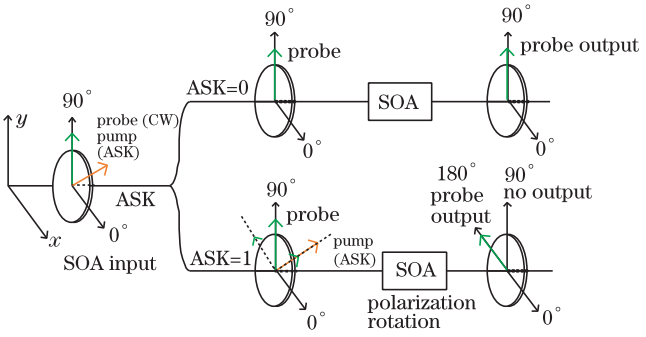

Fig. 2. Principle of the proposed DRZ-FSK transmitter.

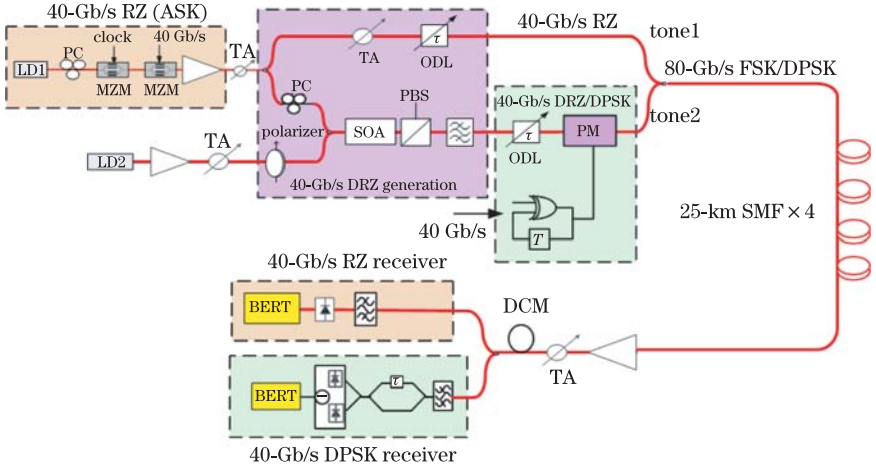

Fig. 3. System setup. LD: laser diode; MZM: Mach-Zehnder modulator; ODL: optical delay line; PM: phase modulator.

realizing a 40-Gb/s RZ signal. The RZ signal is split into two parts by a 3-dB coupler. At the lower tributary, the signal serving as probe is combined with a tunable laser made by Agility Inc. at 1556.3 nm and injected into a 500-m-long SOA. Therefore, the frequency tone spacing (FTS) is about 100 GHz which is enough for 40-Gb/s FSK signal. It is worth noting that crosstalk between two FSK tones can be observed with spectrum overlapping when a small FTS is chosen. Good results can be obtained when the driving current for the SOA is about 200 mA. It is also shown that larger pulse timing jitter can be observed with larger spectral overlapping between the two FSK components. The polarization rotation will occur in the SOA and a DRZ can be obtained after the polarization beam splitter (PBS) and the filter. This signal is re-combined with the upper tributary signal with appropriately tuned attenuation and delay. In this way, an optical DRZ-FSK signal at 40 Gb/s can be generated. The transmission span consists of 100-km SMF with a matching length dispersion compensating module (DCM) in a post-compensation scheme. The span input power is 6 dBm; the DCM input power is 0 dBm.

At the receiver, the frequency discrimination for DRZ-FSK demodulation is achieved by 2 cascaded optical band-pass filters. Good receiver performances can be observed when more than 25 dB suppression ratio is provided between the two FSK tones. This demodulated RZ signal is directly detected. The other tone of DRZ with DPSK is demodulated by a delayed line Mach-Zehnder interferometer (DL-MZI).

For the generation of DRZ signal, the measured optical spectra for the SOA input and output, the DRZ-FSK signal in the back-to-back case and after demodulation are shown in Fig. 4. It is verified that our scheme can effectively convert RZ-ASK to a FSK signal at 40 Gb/s. It should be noted that in RZ-ASK case, one of the FSK tones is a DRZ signal whereas another tone is a RZ signal. The DRZ signal, which is generated through XPR, exhibits spectrum distortion after polarization selection by PBS.

In our scheme, DPSK is modulated based on DRZ which is a larger power tone of the unbalanced FSK. DRZ re-modulated DPSK takes the advantage of optical power in every bit slot, which enables the full re-modulation at

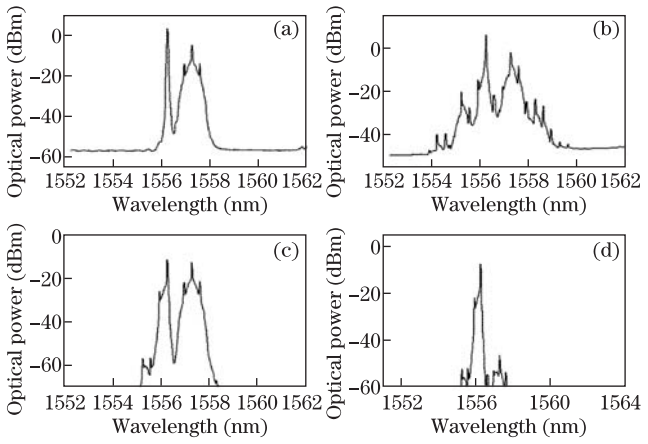

Fig. 4. Measured spectra of (a) SOA input signal, (b) SOA output signal, (c) FSK signal, and (d) the signal after FSK discrimination.

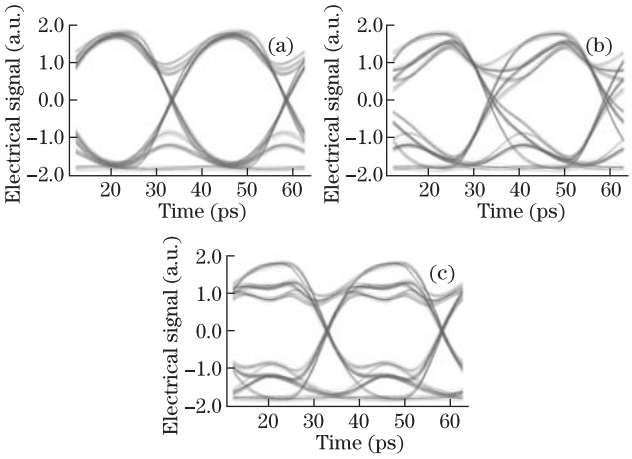

Fig. 5. Eye diagrams of detected DPSK with different clock misalignments to 40-Gb/s DRZ: (a) 0 ps with no misalignment, (b) 5-ps misalignment, and (c) 12.5-ps misalignment.

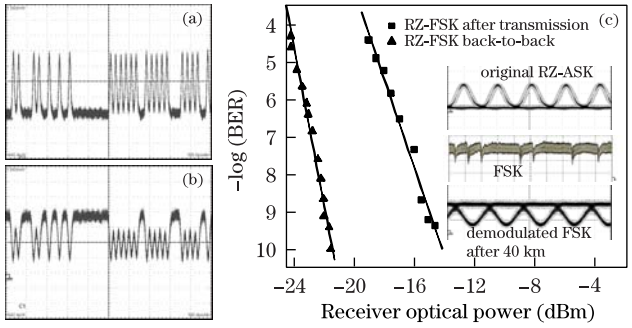

Fig. 6. Measured waveforms for (a) initial RZ signal and (b) DRZ signal; (c) measured BER curves before and after transmission.

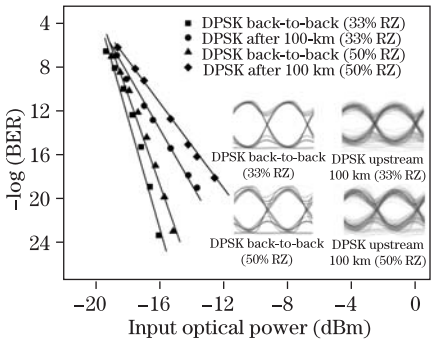

Fig. 7. BER curves of demodulated DPSK for back-to-back and after 100-km transmission uilizing 33% RZ and 50% RZ.

40 Gb/s for both dimensions. However, it is worth noting that the DRZ signal should be accurately adjusted by a delay time to get an optimal clock alignment because DRZ is not power-constant and symmetrical in one bit but has a certain misalignment. The eye diagrams of detected DPSK under back-to-back simulation condition in Fig. 5 show that the signal deteriorates as the clock misalignment increases.

When the attenuation and the time delay on the upper tributary of RZ signal are carefully adjusted, an approximately flat DRZ-FSK/DPSK orthogonal modulation signal waveform can be achieved. Figure 6 shows the optical

waveforms of the initial RZ signal and the DRZ signal. BER curves before and after the transmission link are shown in Fig. 6 (c). Transmission over 100 km results in a power penalty of 6 dB. This relatively large penalty is induced by the residual spectrum distortion, polarization mode dispersion (PMD), and the accumulated noise during SOA processing. The demodulated RZ signal is detected by SHF 47100A V/E converter and the BER is measured by SHF EA44 error analyzer.

Both 33% RZ and 50% RZ are used in our scheme to investigate the effect of duty cycle to the DPSK performance. Figure 7 shows the simulation BER curves of demodulated DPSK for back-to-back and after 100-km transmission utilizing 33% RZ and 50% RZ. All results show good performance of DPSK, which demonstrates the feasibility of our scheme. BER curves for 33% RZ show better system performance compared with 50% RZ with 2-dB enhancement. It is because DRZ is approaching 67% duty cycle for 33% RZ while 50% for the 50% RZ. Thus better receiver sensitivity is obtained when utilizing 33% RZ. Therefore, the corresponding DRZ and DPSK modulation time delay should be about 4 ps and better performances can be obtained. A matching length of dispersion compensation fiber is used to reduce the fiber chromatic dispersion impairment. However, a large power of more than 4 dB is still observed for transmission results due to the residual dispersion, PMD, and fiber nonlinearity. The insets in Fig. 7 show the eye diagrams of back-to-back and after transmission for RZ signals with different duty cycles.

In conclusion, we propose a novel scheme to realize the advanced orthogonal modulation format DRZ-FSK/DPSK based on DRZ generation. The DRZ-FSK is generated by the combination of RZ and DRZ which is converted from RZ using SOA as a nonlinear medium based on nonlinear XPR. The feasibility of the scheme is experimentally demonstrated. The DRZ tone of the 40-Gb/s FSK signal is re-modulated with 40-Gb/s DPSK. The BER results of the total 80-Gb/s DRZ-FSK/DPSK orthogonal modulation signal with a subsequent 100-km SMF transmission link show great potential for future high-speed long-haul fiber networks. BER curves for 33% RZ show better system performance compared with 50% RZ with 2-dB enhancement. The system performances show potential for future high capacity long-haul fiber optical communication.

This work was partially supported by the National Program "973" of China (Nos. 2010CB328300), the National Natural Science Foundation of China (Nos . 600837004 and 60777010), the National "863" Program of China (Nos. 2009AA01Z253 and 2009AA01A347), the Chinese Postdoctoral Science Foundation (No. 20090460593), the Shanghai Postdoctoral Science Foundation (No. 10R21411600), and the Shuguang Fund.

References

1. B. Mukherjee, *Optical WDM Networks* (Springer, New York, 2006).
2. P. J. Winzer and R.-J. Essiambre, J. Lightwave Technol. **24,** 4711 (2006).
3. P. J. Winzer and R.-J. Essiambre, in *Proceedings of the ECOC* Th2.6.1 (2003).
4. A. H. Gnauck, X. Liu, X. Wei, D. M. Gill, and E. C. Burrows, IEEE Photon. Technol. Lett. **16,** 909 (2004).
5. H. Chen, M. Chen, S. Xie, and B. Zhou, in *Proceedings of IEEE Quantum Electronics and Laser Science Conference* CThHH6 (2006).
6. N. Chi and D. Huang, in *Proceedings of IEEE/OSA Optical Fiber Communication Conference* OTuB6 (2007).
7. L. Zhang, C. Yu, X. Xin, and L. Bo, in *Proceedings of IEEE OptoElectronics and Communications Conference* ThP4 (2009).
8. N. Chi, J. Zhang, P. V. Holm-Nielsen, L. Xu, I. T. Monroy, C. Peucheret, K. Yvind, L. J Christiansen, and P. D. Jeppesen, Electron. Lett. **39,** 676 (2003).
9. Y. Shao, L. Chen, S. Wen, Y. Xiao, L. Cheng, H. Xu, and Y. Pi, Opt. Commun. **281,** 3658 (2008).
10. R. Zhou, X. Xin, Q. Zhang, K. Zhao, T. Zhao, and C. Yu, Chin. Opt. Lett. **8,** 464 (2010).
11. L. Liu, L. Wu, F. Zhang, L. Zhu, and Z. Chen, Acta Opt. Sin. (in Chinese) **30,** 676 (2010).
12. Y. Shao, S. Wen, L. Chen, and J. Yu, Chinese J. Lasers (in Chinese) **35,** 1201 (2008).
13. Y. Shao, J. Li, L. Cheng, Y. Pi, S. Wen, and L. Chen, Chinese J. Lasers (in Chinese) **35,** 574 (2008).
14. J. Zhang, W. Fang, C. Hou, X. Liu, X. Zheng, and N. Chi, in *Proceedings of IEEE OptoElectronics and Communications Conference* ThLP62 (2009).
15. Y. Shao, N. Chi, C. Hou, W. Fang, J. Zhang, B. Huang, X. Li, S. Zou, X. Liu, X. Zheng, N. Zhang, Y. Fang, J. Zhu, L. Tao, and D. Huang, J. Lightwave Technol. **28,** 1770 (2010).